HHS Public Access

Author manuscript

Toxicol Appl Pharmacol. Author manuscript; available in PMC 2016 September 07.

Published in final edited form as:

Toxicol Appl Pharmacol. 2011 April 1; 252(1): 1–10. doi:10.1016/j.taap.2011.02.001.

Genotoxicity of carbon nanofibers: are they potentially more or less dangerous than carbon nanotubes or asbestos?

E. R. Kisin[a], **A.R. Murray**[a], **L. Sargent**[b], **D. Lowry**[b], **M. Chirila**[c], **K.J. Siegrist**[b], **D. Schwegler-Berry**[a], **S. Leonard**[a], **V. Castranova**[a], **B. Fadeel**[d], **V.E. Kagan**[e], and **A.A. Shvedova**[a]

[a] Pathology and Physiology Research Branch, Health Effects Lab Division, National Institute for Occupational Safety and Health, Morgantown, WV

[b] Toxicology and Molecular Biology Branch, Health Effects Lab Division, National Institute for Occupational Safety and Health, Morgantown, WV

[c] Exposure Assessment Branch, Health Effects Lab Division, National Institute for Occupational Safety and Health, Morgantown, WV

[d] Division of Molecular Toxicology, Institute of Environmental Medicine, Karolinska Institutet, Stockholm, Sweden

[e] Department of Environmental and Occupational Health, University of Pittsburgh, Pittsburgh, PA

Abstract

The production of carbon nanofibers and nanotubes (CNF/CNT) and their composite products is increasing globally. CNF are generating great interest in industrial sectors such as energy production and electronics, where alternative materials may have limited performance or are produced at a much higher cost. However, despite the increasing industrial use of carbon nanofibers, information on their potential adverse health effects is limited. In the current study, we examine the cytotoxic and genotoxic potential of carbon-based nanofibers (Pyrograf®-III) and compare this material with the effects of asbestos fibers (crocidolite) or single-walled carbon nanotubes (SWCNT). The genotoxic effects in the lung fibroblast (V79) cell line were examined using two complementary assays: the comet assay and micronucleus (MN) test. In addition, we utilized fluorescence *in situ* hybridization to detect the chromatin pan-centromeric signals within the MN indicating their origin by aneugenic (chromosomal malsegregation) or clastogenic (chromosome breakage) mechanisms. Cytotoxicity tests revealed a concentration- and time-dependent loss of V79 cell viability after exposure to all tested materials in the following sequence: asbestos>CNF>SWCNT. Additionally, cellular uptake and generation of oxygen radicals was seen in the murine RAW264.7 macrophages following exposure to CNF or asbestos

Correspondence should be addressed to: A.A. Shvedova (AShvedova@cdc.gov; 1095 Willowdale rd, Morgantown, WV 26505; phone: 304-285-6177; fax: 304-285-5938).

DISCLAIMER

The findings and conclusions in this report are those of the authors and do not necessarily represent the views of the National Institute for Occupational Safety and Health.

but not after administration of SWCNT. DNA damage and MN induction were found after exposure to all tested materials with the strongest effect seen for CNF. Finally, we demonstrated that CNF induced predominately centromere-positive MN in primary human small airway epithelial cells (SAEC) indicating aneugenic events. Further investigations are warranted to elucidate the possible mechanisms involved in CNF-induced genotoxicity.

Keywords

carbon nanofibers; genotoxicity; oxidative stress; DNA damage; cytotoxicity

INTRODUCTION

Carbon nanofibers (CNF) are a carbonaceous nanomaterial used mainly in advanced composite materials to improve strength, stiffness, durability, electrical conductivity, or heat resistance (Darne et al., 2010). CNF cost significantly less to produce than carbon nanotubes (CNT) and therefore offer significant advantages over nanotubes for certain applications, providing a high performance to cost ratio. The broad utility of nanomaterials is resulting in increased levels of production, with increased human exposure and the potential for release of these novel materials in the environment. Therefore, close attention to toxicological issues related to nanoparticles, including various fibrous nanomaterials, is of paramount importance (Shvedova et al., 2010).

CNF lie between conventional milled carbon fibers (5–10 μm diameter) and single-walled carbon nanotubes (SWCNT) (1–10 nm diameter) in terms of size. Hence, the typical diameters of CNF is on the order of 50–200 nm (Ku et al., 2006) with lengths from tens of micrometer to several centimeters, and an average aspect ratios of >100. Structurally, CNF are more similar to multi-walled carbon nanotubes (MWCNT): both materials possess hollow cores and display either discrete or bundled fibrous morphologies (Ku et al., 2006; Wang et al., 2007). In contrast, SWCNT are less rigid structures and have a strong tendency to form nonfibrous bundles and ropes (Maynard et al., 2007; Shvedova et al., 2005). The primary characteristic that distinguishes CNF from CNT resides in graphene plane alignment: if the graphene plane and fiber axis do not align, the structure is defined as a CNF, but when parallel, the structure is considered as a CNT (ISO/TS 27687:2008, 2008).

Although carbon nanotubes have been shown to be susceptible to enzymatic biodegradation by horseradish peroxidase and the human myeloperoxidase expressed in neutrophils (Allen et al., 2009; Kagan et al., 2010), these materials may remain in the body for long periods of time following exposure. Indeed, the durability and physical characteristics (high aspect ratio) of carbon nanotubes resemble those of asbestos and suggest similar toxicity for carbon nanotubes and asbestos fibers (Muller et al. 2008, Poland et al., 2008). The critical factors associated with asbestos pathogenicity and carcinogenicity are biopersistence, pulmonary penetration, fiber length/diameter (aspect ratio), and the ability to generate reactive oxygen species (ROS) (Shukla et al., 2003; Vallyathan et al., 1998). Genotoxic effects associated with these phenomena or occurring independently are also likely to play an important role for the adverse effects of asbestos.

The human health hazards associated with exposure to carbon nanoparticles have not been fully investigated, especially their potential for genotoxicity and carcinogenicity. Damage to DNA is the one of the most important effects since an increased genetic instability is associated with cancer development. Compared to known genotoxic compounds, nanoparticles are unique because of their behavior and physicochemical characteristics that are completely different from fine-sized particles of similar composition (Knaapen et al., 2004). Genotoxic activities may result from direct interaction of particles with the genetic material or secondary damage resulting from particle-induced reactive oxygen species (ROS) production. Both pathways may relate to surface properties, the presence of transition metals, intracellular iron mobilization, or lipid peroxidation processes. Other aspects relevant to primary genotoxicity are particle size, shape, particle uptake, and the presence of mutagens carried with the particles (Schins, 2002). Currently, numerous studies have focused on genotoxic properties of carbon nanotubes showing that SWCNT or MWCNT may induce DNA damage, micronuclei formation, disruption of the mitotic spindle, and induction of polyploidy (Asakura et al., 2010; Jacobsen et al., 2008; Kisin et al., 2007; Li et al., 2006; Lindberg et al., 2009; Muller et al., 2008; Pacurari at al., 2008a, 2008b; Patlolla et al., 2010; Sargent et al., 2009, 2010; Schrand et al., 2008; Yamashita et al., 2010; Zhu et al., 2007).

Surprisingly, despite the current widespread use of carbon nanofibers, toxicological studies have mainly focused on carbon nanotubes, and only a few studies have evaluated different carbon nanofibers and their toxicity (Brown et al., 2007; Grabinski et al., 2007; Lindberg et al., 2009; Magrez et al., 2006; Price et al., 2004). Little or no research has been conducted to date on genotoxicity of CNF. In the present study, we investigated whether exposure to Pyrograf III CNF had the potential to induce genotoxicity *in vitro*, as determined using the comet assay and micronucleus test. Additionally, in order to approach the mechanisms involved, we studied the clastogenic and/or aneugenic effects of CNF using the pancentromeric fluorescent probe in human small airway epithelial cells (SEAC). For comparison, the cytotoxic and genotoxic potential of crocidolite asbestos and SWCNT were also evaluated. The present studies reveal differences in the genotoxic potential for the three fibrous nanomaterials, with CNF displaying the most prominent effect.

MATERIALS and METHODS

Particles

CNF were purchased from Pyrograf® Products, Inc. Vapor grown carbon nanofibers (PR-24, LHT grade) were heat treated (up to 3000°C) to graphitize chemically vapor deposited carbon present on the surface of Pyrograf®-III and to remove iron catalyst. SWCNT (CNI Inc., Houston, TX) produced by the high pressure CO disproportionation process (HiPco) technique, and purified by acid treatment to remove metal contaminates (Gorelik et al., 2000) were used in this study. A UICC standard crocidolite asbestos was used as a positive well characterized control in the study. Chemical analysis of total elemental carbon and trace metal (iron) were performed at the Chemical Exposure and Monitoring Branch (DART/NIOSH, Cincinnati, OH). Elemental carbon was assessed according to NIOSH Manual of Analytical Methods (NMAN) (Bronikowski et al., 2001), while metal content (iron) was

analyzed using nitric acid dissolution and inductively coupled plasma-atomic emission spectrometry (ICP-AES) performed according to NMAM method 7300 for trace metals. For purity assessment of CNF and SWCNT, several standard analytical techniques were used including thermo gravimetric analysis with differential scanning colorimetry (TGA-DSC), thermo-programming oxidation (TPO), and Raman spectroscopy (Arepalli et al., 2004; Birch, 2003; Dresselhaus et al., 2004). Specific surface area was measured at −196° C by the nitrogen absorption–desorption technique (Brunauer Emmet Teller method, BET) using a SA3100 Surface Area and Pore Size Analyzer (Beckman Coulter Inc, Fullerton, CA). To obtain more homogeneous and dispersed suspensions, CNF, SWCNT and asbestos were ultrasonicated (30s × 3 cycles). SEM showed that sonication significantly improved the dispersion of nanoparticles.

Raman spectroscopy

Raman spectroscopy was employed for morphology characterization of the test nanoparticles. 100 μl of each sample were placed on a microscope slide on which a 9 mm silicon well was glued in order to keep the solution confined. The microscope slides were dried in air and placed under the laser beam for Raman analysis. Raman spectra were recorded in backscattering geometry, using a Horiba Jobin-Yvon M1250 spectrometer equipped with a liquid nitrogen-cooled CCD detector. The samples were excited with 514.5 nm from an argon ion laser. An Olympus BH2 confocal microscope with an 80× objective was used to focus the laser beam to about 5 to 10 μm and to collect the scattered light. Calibration of the instruments was done by checking the position of the Si band at 521 cm^{-1}. Raman spectra from CNF and SWCNT were analyzed by calculating the R parameter and the graphite mole fraction. These two parameters are often used to characterize the morphology and purity of the materials (Rinaudo et al., 2004). The R parameter is defined as the ratio of D band over G band (Figure 1A and B), $R = I_D/I_G$. To a first approximation, I_D and I_G are supposed to have the same proportionality coefficient with non-graphite mole fraction - χ_D and the graphite mole fraction - χ_G, respectively. Then, χ_G can be estimated to be $I_G/(I_D+I_G)$, or $1/(1+R)$ (Wang et al., 2003). The decrease of parameter R implies the increase of graphite mole fraction χ_G in the fibers.

Cell culture

Chinese hamster lung fibroblast (V 79) cells (American Tissue Culture Collection, ATCC, Manassas, VA) were seeded in MEM medium with Earle's salts and L-glutamine and supplemented with pen-strep antibiotics (2%) and 10% fetal bovine serum. Cultures were maintained at 37° C in a humidified atmosphere containing 5% CO_2. To assess *in vitro* cellular responsiveness to CNF, asbestos or SWCNT, V79 cells were treated (0–48 μg/cm^2 [corresponds to 0–172 μg/ml], 3–24 h, at 37°C). Following exposure, measurements of cytotoxicity and genotoxicity (comet and micronucleus assays) were conducted. RAW 264.7 macrophages (ATCC) were grown in DMEM supplemented with 10% heat inactivated FBS, 100 units/ml penicillin and 100 μg/ml streptomycin in a humidified atmosphere (5% CO_2 plus 95% air) at 37°C. Following cells exposure to CNF, asbestos or SWCNT (0.12 mg/10^6 cells or 0.24 μg/cm^2), assessments of ROS production and changes in cell morphology were performed. Human primary small airway epithelial cells (SAEC) were utilized for the analysis of the micronuclei after exposure to CNF. SAEC were obtained and cultured

following manufacturer's directions using Cabrex media (Lonza, Walkersville, MD). Following cells exposure to CNF (2.4 and 24 μg/cm^2), chromatin pancentromeric signals within the MN were determined.

Scanning Electron Microscopy (SEM)

CNF, asbestos or SWCNT were diluted in double-distilled water and filtered with a 0.4 μm nucleopore filter. The filter was attached with double-stick carbon tape on an aluminum mount and sputter coated with gold/palladium. Images were collected on a JEOL 6400 scanning electron microscope.

Transmission Electron Microscopy (TEM)

The sample was diluted in double-distilled filtered water. The solution was then mixed and a drop placed on a formvar –coated copper grid and allowed to air dry. Images were photographed on a JEOL 1220 transmission electron microscope.

ESR measurements

Electron spin resonance (ESR) spin trapping was used to examine free radical generation by CNF, asbestos or SWCNT in RAW264.7 macrophages. DMPO spin trapping agent was used for radical detection. All measurements were performed using a Bruker EMX with a HS cavity. Instrument settings were as follows: microwave power, 20 mW; modulation amplitude, 1.0 G; conversion time, 0.6 s; time constant, 1.3 s. Hyperfine coupling constants were determined using the WinSim program of the NIEHS public EPR software tools package, which is available over the Internet (http://epr.niehs.nih.gov/). The relative radical concentration was estimated by measuring the peak-to-peak height (mm) of the observed spectra.

Cytotoxicity assay

V79 cells were treated with CNF, asbestos or SWCNT (suspended MEM medium without phenol red and FBS supplementation) at different doses (0, 3, 12 or 48 μg/cm^2) for 3 and 24 hr. After incubation, cells were washed twice with PBS, pH 7.4, and harvested using a cell scraper. Cell viability was evaluated immediately after exposure using trypan blue staining. The cell suspension was mixed with an equivalent volume of 0.4% trypan blue solution, and cell counting was performed using hemacytometer with a light microscope. Results were expressed as % of viable cells.

Comet assay

V79 cells were seeded into 25 cm^2 flasks (2.0 × 10^6/flask) with 5 ml of MEM medium supplemented with 10% FBS and 2% pen-strep antibiotics. After cells were attached, medium was removed and replaced with suspensions of CNT, asbestos or SWCNT in MEM medium without phenol red and FBS supplementation at concentrations of 0, 3, 12 or 48 μg/cm^2 or N-methyl-N-nitroso-N-nitrosoguanidine (MNNG) as a positive control. After 3 or 24 hr of exposure, cells were washed with Mg^{++} and Ca^{++} free balanced salt solution (HBSS). A cell scraper was used to remove cells from the flask. Each sample was adjusted to a concentration of 1×10^6 cells/ml, frozen in liquid nitrogen and stored at −70±10° C until

shipping to HELIX3 Inc. (Morrisville, NC) for Comet assay analysis (Karlsson, 2010). A total of 100 randomly captured cells from each sample/slide were examined. All experiments were repeated three times.

Micronucleus assay

Cells were seeded into 25 cm^2 flasks (1.0×10^6/flask) with 5 ml of complete medium (MEM medium supplemented with 10% FBS and 2% pen-strep) and cultured overnight. The medium was removed and replaced with suspensions of CNF, asbestos or SWCNT in MEM medium without phenol red and FBS supplementation at concentrations of 0, 3, 12 or 48 μg/cm^2 for 24 hr. Cells were rinsed with phosphate buffered solution (PBS), and incubated in 5 ml of complete medium for 24 hr. A cell scraper was used to remove cells from the flask. Each sample was adjusted to a concentration of 1×10^6 cells/ml, frozen in liquid nitrogen and stored at −70±10° C prior to shipping to HELIX3 Inc. (Morrisville, NC) for MN analysis. MNNG was used as a positive control in each MN test.

Fluorescence *in situ* hybridization

Primary human respiratory epithelial cells (SAEC) isolated from the small airway of a normal human donor were examined to determine the response of a normal cell population to CNF exposure. SAEC were obtained and cultured following manufacturer's directions using Cabrex media (Lonza, Walkersville, MD). Metaphase chromosome spreads were prepared and the chromosomes were banded following methods outlined previously (Wiley et al, 1984). Analysis of banded chromosome preparations confirmed that the SAEC cells have a normal diploid 46 XY karyotype. The normal diploid karyotype was necessary for the determination of potential aneuploidy induction following exposure. Fluorescence *in situ* hybridization (FISH) using human pancentrometric probe was described previously by Decordier et al., 2002. Primary SAEC were treated with 2.4, or 24 μg/cm^2 of CNF for 24h. After cells were fixed, FISH was performed with a directly FITC-labelled human pancentromeric probe (Thermo Fisher Scientific Inc., Waltham, MA). For FISH analysis a minimum 300 cells were scored by two independent observers for each treatment and dose. The MN were examined for the presence of FISH signals and were classified as centromere positive or centromere negative. Zeiss Axiophot microscope (Carl Zeiss) equipped with Applied Imaging software was used. As we were using primary human cells, a background rate of MN in control samples was not detectable.

Statistical analysis

Results were compared by One Way ANOVA using the All Pairwise Multiple Comparison Procedures (Holm-Sidak method). All results are presented as mean ± SEM. *P* values of less than 0.05 were considered to be statistically significant.

RESULTS

Characterization of fibrous nanomaterials

To characterize the Pyrograf CNF used in this study, chemical analysis was performed by NMAM #5040 and ICP-AES and revealed that CNF were comprised of 98.6 weight % elemental carbon, and iron levels were approximately 1.4 weight %. Raman spectroscopy

was used to confirm the identity of CNF and to estimate the graphite mole fraction. Figure 1A shows representative Raman spectra recorded from CNF. Two main bands are identified as typically observed for any graphite-base materials. The disorder band (D band) around 1350 cm^{-1} comes from the disordered sp^2 bonding carbon atoms (Dresselhaus et al., 1999) and is attributed to amorphous carbon and impurities. The graphite-like band (G band) around 1590 cm^{-1} is due to ordered sp^2 bonding carbon atoms stretching tangentially to the fiber. The estimated values for the graphite mole fraction for CNF show that approximately 50% of the material is in the graphite structure (Table 1), which is considered to be a high degree of graphitization and purity for carbon nanofibers. The CNF diameters in the samples ranged from 60–150 nm and the specific surface area of CNF was 35–45 m^2/g. The length of the individual CNF is approximately 30–100 μm as confirmed by SEM (Figure 2A).

To characterize HiPco SWCNT, chemical analysis was performed by NMAM #5040 and ICP-AES and revealed that SWCNT were comprised of 99.7 weight % elemental carbon, and iron levels were approximately 0.23 weight %. The Raman spectrum of the SWCNT sample (Figure 1B) shows distinct bands around 200 cm^{-1} from the radial breathing mode (RBM) and the D and G bands at 1350 and 1590 cm^{-1}, respectively. Analysis of the spectra indicated that the nanotube diameters in the samples ranged from 1–4 nm. Comparative analytical data obtained by TGA-DSC, TPO and Raman spectroscopy revealed that more than 95% of carbon content in the SWCNT Hipco product was accountable as carbon nanotubes. The specific surface area of SWCNT was 1040 m^2/g. The length of the individual SWCNT is approximately 1–3 μm as determined by SEM (Figure 2B).

Chemical analysis of crocidolite asbestos revealed that iron levels were approximately 18 weight %. The Raman spectrum of asbestos sample (Figure 1C) presents all the specific vibrational bands due to metal – oxygen modes at low frequencies and the silicon – oxygen (Si-O) modes at higher frequencies, as indicated on the plot (Bard et al., 1997; Rinaudo et al., 2004) with the strongest band at 969 cm^{-1} due to non-bridging Si-O stretching mode. The surface area of asbestos is 8.3 m^2/g and the length of the individual asbestos fiber is approximately 0.6–12 μm as confirmed by SEM (Figure 2C).

Cellular uptake and generation of reactive oxygen intermediates

To assess nanoparticles uptake and cell damage, the murine RAW264.7 macrophage cell line was utilized. TEM of RAW264.7 macrophages incubated with 24 $\mu g/cm^2$ of CNF (24h, 37 °C) revealed ultra-structural changes in cell morphology with fibers penetrating intracellular structures (Figure 3B). In particular, nucleus, mitochondria, tonofilaments, and other cytoplasmic organelles were altered with the strongest changes evident after exposure to CNF (Figure 3B). Exposure of RAW264.7 macrophages to SWCNT also resulted in ultra-structural changes in cell morphology. The macrophages were found to internalize CNF and asbestos but not carbon nanotubes (Figure 3C). RAW264.7 macrophages exposed to 24 $\mu g/cm^2$ of asbestos showed normal architecture in spite of the presence of fibers (Figure 3D).

To determine the extent to which CNF, asbestos or SWCNT are able to generate free radicals, we utilized the ESR spin trapping technique. Formation of free radicals was determined in RAW264.7 macrophages after a 5 min of exposure to CNF, asbestos or

SWCNT. Figure 4B showed ESR spectra of a DMPO spin-trapped ·OH radical after exposure with CNF (120 μg/10^6 cells). This spectrum consists of a 1:2:2:1 quartet with splittings of $a^H = a^N = 14.9$ G, where a^H and a^N denote hyperfine splittings of the α-hydrogen and the nitroxyl nitrogen, respectively. On the basis of these coupling constants, the 1:2:2:1 quartet was assigned to DMPO/·OH adduct. Addition of H_2O_2 dramatically increased the DMPO/·OH adduct signal (Fig. 4C), while addition of catalase, an H_2O_2 scavenger, to the incubation system decreased the generation of ·OH radical (Fig. 4D). Addition of the metal chelator, deferoxamine (DFO), also strongly suppressed the DMPO/·OH signal (Fig. 4E). These results suggested that ·OH generated during exposure of RAW264.7 macrophages to CNF was formed via a metal-dependent Fenton reaction which may cause oxidative stress, cell damage and genotoxicity. Figure 4F showed strongest significant intensity of ESR signals after exposure with asbestos (4-fold over control) or CNF (2.5-fold over control), while signal after SWCNT exposure was hardly discernable.

Cytotoxicity assessment of fibrous nanomaterials

The cytotoxic potential of CNF, asbestos and SWCNT was determined after exposure of V79 cells in MEM without phenol red or FBS supplementation, to avoid interaction of nanomaterials and medium components, particularly serum (Doak et al., 2009). Following 3 or 24h of exposure, cells were counted using trypan blue dye exclusion. This direct cell counting method was chosen to avoid any artifactual results due to the interaction of the nanoparticles and the dyes that are commonly used in automated cell viability assays (Doak et al., 2009). The results show a significant decrease in cell viability of CNF-, asbestos- or SWCNT-exposed V79 cells with increasing dose and exposure time (Figure 5). Exposure with the two highest concentrations (12 and 48 μg/cm^2) for 24h resulted in significantly stronger cytotoxic effects for asbestos (38% and 51.5% loss of viability, respectively) and CNF (26.5% and 36% loss of viability, respectively) in comparison with SWCNT (10% and 22%, respectively). Loss of viability after exposure of cells to all tested materials for 3h also revealed the same rank order of potentcy: asbestos>CNF>SWCNT. No cytotoxic effect was found at the lowest concentration (3 μg/cm^2) used in the study. As high loss of viability may interfere with accurate evaluation of genotoxicity responses, we excluded 48 μg/cm^2 of asbestos from further examination of DNA damage and MN induction. N-methyl-N-nitroso-N-nitrosoguanidine (MNNG), used as a positive control for DNA damage, showed no cytotoxicity at the chosen conditions.

Genotoxicity assessment of fibrous nanomaterials

To evaluate whether CNF, asbestos or SWCNT induce DNA damage, the Chinese hamster lung fibroblast (V79) cells were exposed to different doses of tested fibrous materials (0, 3 or 48 μg/cm^2, for 3 or 24 hr) in MEM without phenol red and FBS. The results of the Comet assay are expressed as % migrated DNA (Figure 6A), tail lengths (Figure 6B), and olive tail moments (Figure 6C). A short-term CNF treatment for 3 hr led to significant DNA damage (106%, 48% and 201% increase of DNA migration, tail length and olive tail moment, respectively, in comparison with vehicle-treated cells) at the highest tested dose of 48 μg/cm^2. A short-term CNF treatment (48 μg/cm^2) also led to the strongest DNA damage (95%, 43% and 190% increase of DNA migration, tail length and olive tail moment, respectively) in comparison to SWCNT treatment. More prolonged treatment with CNF for 24 hr

increased all parameters of DNA damage in a concentration-dependent way. A 24 hr exposure to 3 μg/cm^2 of CNF significantly increased the level of migrated DNA, tail length and olive tail moment by 45%, 68%- and 102%, respectively, while treatment with 48 μg/cm^2 CNF produced a non-significant elevation in these parameters by 118, 88% and 376%, respectively. A long-term SWCNT treatment (48 μg/cm^2) led to significant DNA damage. No significant differences in DNA damage were found between CNF and SWCNT following long-term 24h treatments. A comparison of CNF and asbestos treatments showed no differences in DNA damage at any time of exposure. The highest dose of asbestos (48 μg/cm^2) was not assessed for DNA damage to avoid interference of cell death (cytotoxicity > 50%) with accurate evaluation of the genotoxic responses detectable in viable cells. DNA damage in the positive control group (cells treated with 0.05 μg/cm^2 MNNG) increased the level of migrated DNA by 85±24% at both times of exposure (data not shown).

In order to examine the effect of CNF, asbestos or SWCNT on the stability of chromosomal DNA, MN induction was evaluated in cells. Micronuclei are a result of chromosomal breakage and/or mitotic spindle damage evaluated in interphase cells. The Chinese hamster lung fibroblast (V79) cells were exposed to CNF, asbestos or SWCNT (0, 3, 12, or 48 μg/cm^2) for 24 hr in MEM without phenol red or FBS. To allow damaged cell to form micronuclei in the next interphase, cells were removed from the tested materials containing medium and grown for an additional 24 hr. The results of 3 replicate assays indicate dose-dependent increase in MN induction after exposure to all tested particles (Figure 7A). Low concentration (3 μg/cm^2) of CNF or asbestos led to elevated but not significantly different induction of MN. Exposure with 12 μg/cm^2 of CNF, asbestos or SWCNT showed significant induction (2.9-, 2.3- or 1.9-fold, respectively) of MN in comparison to control (PBS) while the highest dose of 48 μg/cm^2 of CNF or SWCNT induced a significant increase (2.5- or 2.2-fold, respectively) in the frequency of MN.

To determine whether MN formed upon exposure to CNF comprised an entire chromosome (aneugenic event) or an acentromeric chromosome fragment (clastogenic event), we used a pancentromeric probe. As this probe is not available for mice chromosomes, a human pancentromeric probe was used in a human SEAC to further investigate the mechanisms involved. SEAC (500 cells) were scored for the presence or the absence of a hybridization signal from the pancentromeric probe (Figures 7B, 7C and 7D). Although the methodology was different from that used in Figure 7A, we observed a similar trend for the formation of MN in response to CNF exposure. CNF induced an increased number of both centromere-positive and -negative MN with prevailing of aneugenic events (80%). Additionally, we observed MN with both single centromere (C1+MN) and two or more centromeres (Cx +MN) visible signals (Figure 7C). As we were using primary human cells, background rate of MN in control samples was not detectable. Doses for this experiment were chosen based on the viability of SEAC (data not shown) and only non- or low cytotoxic concentrations were used. Moreover, we could observe CNF within the nucleus of SEAC (Figures 7C and 7D). All these results confirm that CNF are able to induce genotoxicity and provide evidence that these particles induce aneugenic as well as clastogenic events.

DISCUSSION

There is currently a concern that human exposure to fibrous carbon nanomaterials will produce pathological reactions similar to those of asbestos fibers. The causal association between exposure to asbestos fibers and development of lung cancer is well documented. Furthermore, inflammation and pulmonary fibrosis have been associated with an increased risk for lung cancer (Hubbard et al., 2000; Knaapen et al., 2004). Since previous studies have documented pulmonary inflammation and fibrosis induced by carbon nanotubes (Shvedova et al., 2009), assessment of the genotoxic potential of carbon nanomaterials is important. Since CNF have a high aspect ratio and biodurability that are characteristic features of amphibole asbestos (crocidolite), we may hypothesis that CNF may behave like asbestos. The ability of CNF to induce ROS production, cytotoxicity and genotoxicity in cellular systems was investigated in this report, and compared with the effects of SWCNT or crocidolite asbestos exposures.

Surprisingly, limited studies have evaluated the toxicity of different carbon nanofibers. Our finding of CNF-induced cytotoxicity and particles engulfment by the cells were similar to those demonstrated by Price et al. (2004) providing evidence of time- and dose-dependent CNF (diameter: 60–100 nm) cytotoxicity using human osteoblast CRL-11372 cells with particles taken up into cells and enclosed in vacuoles. Magrez et al. (2006) also studied cellular toxicity of different carbon nanoparticles, including CNF, with different aspect ratios. This work indicated a stronger toxicity of CNF (aspect ratio: 30–40) as compared to MWCNT (aspect ratio: 80–90) in H596 lung tumor cells. In line with the latter observations, we found that the cytotoxicity induced by CNF (aspect ratio: 500) is significantly stronger than SWCNT (aspect ratio: 1000). In contrast, Grabinski et al. (2007) reported that CNF (diameter: 100nm, iron: 0.25%) induced very minor cellular toxicity when compared to SWCNT or MWCNT with unchanged morphology of mouse keratinocytes (HEL-30).

All three tested materials used in the study were found to be genotoxic in Chinese hamster lung fibroblast V79 cells, as measured by the alkaline comet assay and the micronucleus assay. Dose-dependent increases in the frequency of DNA damage were seen in the comet assay after exposure to CNF, asbestos or SWCNT. CNF exposure induced the same level of DNA damage as asbestos at the doses tested but had a stronger effect in comparison to SWCNT treatment. Exposure of cells to CNF, asbestos or SWCNT caused about the same level of MN induction. Significantly different results were obtained in both tests even at non-cytotoxic doses. Additionally, we found that CNF act as an aneugenic and clastogenic agent simultaneously with prevailing incidence of positive chromatin pan-centromeric signals within the MN. In a recent study, Lindberg et al. (2009) observed that graphite nanofibers induced DNA damage (comet assay) at all doses used (1–100 μg/cm^2) following 24h of exposure in human bronchial epithelial cells (BEAS-2B). In our study, significant DNA damage was induced as early as 3h of exposure at 48 μg/cm^2 while 3 μg/cm^2 of CNF caused significant DNA damage after 24h of treatment. Positive but not dose-dependent effects on MN induction were detected by Lindberg et al. (2009) at doses of 5 μg/cm^2 and 20 μg/cm^2 after longer exposures (48 or 72h) while in our experiments significant MN induction was observed after 24h of exposure starting at 12 μg/cm^2.

Genotoxicity is expressed as various types of DNA damage (DNA adducts, alkali-liable sites, strand breaks) and mutations, ranging from gene to structural or numerical chromosome changes (aneploidy and polyploidy) (Kirsch-Volders et al., 2002; Mateuca et al., 2006; Muller et al., 2008). Two processes are implicated in the induction of genotoxic effects by nanoparticles with low solubility: primary genotoxicity depends on the intrinsic activity of the particles, whereas secondary genotoxicity is associated with the inflammatory events elicited by the particles (Schins, 2002). The ability of particles to trigger ROS generation is known to play a major role in primary genotoxicity. These reactive species arise at the surface of the particles or may be mediated by the chemical constituents of the particles, including the presence of transition metals such as iron (Ding et al., 2002; Manning et al., 2002). In our study, we demonstrated a CNF-induced increase in the frequency of DNA damage as measured by comet assay. Cellular uptake and ROS generation are likely to be the major factors involved in the DNA damage process. Excessive generation of ROS usually leads to an imbalance between oxidant and antioxidant mechanisms, manifested through oxidative stress. When the balance is in the favor of ROS production, it can interact or modify DNA. As inducer of radicals, CNF is less potent than asbestos but much stronger than SWCNT. Additionally, depletion of glutathione induced by CNF was comparable to asbestos exposure and significantly stronger than SWCNT (data not shown). Even though, CNF generated less radical species than asbestos, we show that DNA damage induced by CNF was as strong as that induced by asbestos. Crocidolite, a well documented pulmonary carcinogen, induced great levels of ROS, leading to enhanced DNA damage. Msiska et al. (2010) demonstrated that crocidolite asbestos induced DNA double-strand breaks (DSBs) *in vitro*. It is known that DNA DSBs are a major type of DNA damage that can lead to translocations and chromosomal instability. While they are less common than single-strand breaks, their repair is more difficult.

The two basic phenomena lead to the formation of MN in mitotic cells: chromosome breakage and dysfunction of the mitotic apparatus. In genotoxicity testing, it is critical to understand whether a MN inducer acts via clastogenic or aneugenic (or both) mechanism. Our experiments indicate that CNF-related genotoxicity is the result of both aneugenic and clastogenic events with prevailing incidence of numerical abberations. It is known that crocidolite asbestos induced MN with structural aberrations affecting the centric/pericentric regions and numerical changes in chromosome numbers (Dopp et al., 1997). Additionally, Muller et al. (2008) demonstrated the potential of MWCNT to induce both events with majority being aneugenic changes. Several potential mechanisms may explain the aneugenic effect of CNF, including a physical interaction of nanofibers (since nanofibers shown to be internalized by the cells) with components of the mitotic spindle during cell division or the interaction with proteins directly or indirectly involved in chromosome segregation (e.g. tubulin, actin). This may lead to genetic instability, in the form of micronuclei and chromosomal imbalances, or aneuploidy in daughter cells. Aneuploidy occurs when replicated chromosomes fail to accurately segregate between the two daughter cells leading to the production of cells with an abnormal number of chromosomes. Aneugens could act on different cell targets, but disturbance of the mitotic spindle (kinetochores, centrosomes, microtubules and the anaphase promoting complex) is most often reported. Indeed, SWCNT and crocidolite asbestos have been found to induce chromosomal aneuploidy and disturb the

mitotic spindle (Sargent et al., 2009; Yegles et al., 1995). The interaction of an aneugen with its target receptor often exhibits a characteristic dose-response pattern (Aardema et al., 1998), while aneuploidy induction through the inhibition of spindle function does not involve the direct interaction of the agent with DNA and possibly may explain the absence of dose–response for the CNF-induced aneugenic MN in our study. Moreover, aneugenic events leading to MN containing a single centromere (C1+MN) and two or more centromeres (Cx+MN) may arise through different pathways (Iarmarcovai et al., 2006). Chromosome migration impairment would lead to increased C1+MN frequency whereas centrosome amplification would induce Cx+MN with three or more centromeric signals. In this study, we observed MN with both C1+MN and Cx+MN visible signals, indicating different mechanisms involved in the aneugenic events induced by CNF.

Several hypotheses can be suggested to account for the clastogenic effect of CNF, including the formation of adducts and/or damage at the level of DNA or chromosomes. The prevailing mechanism proposed to explain chromosome breakage is related to the generation of ROS. Iron present at the surface of particles is implicated in the pathogenicity of fibers, and thought to be mobilized in cellular systems, thus initiating the ROS generation via a Fenton reaction. The presence of metallic contaminants in CNF such as transition metals (1.4% Fe) would fit with this hypothesis since we found that CNF generate ROS in a cellular model. In the recent study, Pietruska et al. (2010) demonstrated that crocidolite asbestos (1.0–5.0 μg/cm^2) induced primarily clastogenic micronuclei in human lung epithelial cells. Clastogenic micronuclei arise from chromosome breaks, and the ability of asbestos to generate DNA breaks is strongly linked to the presence of fiber-associated iron and ROS generation (Shukla et al., 2003). Crocidolite asbestos contains up to 27% iron by weight (18% in our study), while CNF utilized in the study contain only 1.4%. Therefore, the different proportions of clastogenic and aneugenic micronuclei generated by crocidolite asbestos and CNF may reflect their different iron contents. Nevertheless, other particle properties such as size and shape may also be important, as this may impact the ability of phagocytic cells to handle the materials. It has been shown that when macrophages attempt to phagocytose long fibers such as crocidolite asbestos the process of phagocytosis is frustrated, resulting in the release of ROS (Goodlick and Kane, 1986; Hill et al., 1995). On the other hand, we reported previously that macrophages are not effective at engulfing or phagocytozing purified SWCNT (0.23% iron) (Shvedova et al., 2005), while the presence of the contaminating iron in SWCNT was found to be important in determining redox-dependent responses of macrophages (Kagan et al., 2006). In line with this, our examination of RAW264.7 macrophages incubated with CNF revealed ultra-structural changes in cell morphology with fibers penetrating the cells. SWCNT were engulfed by macrophages to a much lesser extent as compared to CNF or asbestos. Brown et al. (2007) demonstrated the negative impact of CNF on the phagocytic activity of human mononuclear cells (THP-1), and we have shown that SWCNT may suppress the phagocytic activity of primary human macrophages (Witasp et al., 2009). This could provide a partial explanation for the “frustrated” phagocytosis phenomenon.

A direct interaction between particles and the genetic material should be also considered. Indeed, SWCNT has been shown to enter the cell by passive diffusion and endocytosis (Doak et al., 2009) and have been observed in the nucleous in interphase cells (Pantarotto et

al., 2004; Sargent et al., 2008). Li et al. (2005) suggested that CNT are efficient in interacting with biomolecules with similar dimensions, such as DNA. Furthermore, bundles of SWCNT are similar to the size of microtubules and may be incorporated into the mitotic spindle rather than the physical interference of the spindle that occurs with asbestos fibers (Sargent et al., 2009). Thus, SWCNT may disrupt the mitotic spindle in dividing cells and induce formation of anaphase bridges among the nuclei, which is a consequence of the misrepair of multiple induced double strand breaks of the DNA (Cveticanin et al., 2010). Due to a larger diameter of CNF, mechanisms of cellular uptake and possible mitotic spindle disruption could be different from those induced by SWCNT.

In conclusion, all three fibrous nanomaterials tested in the present study were genotoxic *in vitro*. Genotoxicity of CNF was found to be comparable with asbestos and stronger than SWCNT. Our results further support the hypothesis that nano-sized fibers may cause genotoxicity via two different mechanisms: first by production of ROS, which in turn react readily with DNA, and second, by interfering physically with DNA/chromosomes and/or the mitotic apparatus. Different amount of surface iron of the nanofibers could be correlated with their propensity to trigger ROS production and subsequently with the toxic responses. Further investigations are warranted to elucidate the genotoxic properties of CNF *in vitro* and *in vivo* and the possible mechanisms involved in such genotoxicity.

Supplementary Material

Refer to Web version on PubMed Central for supplementary material.

Acknowledgments

This work was supported by NIOSH OH008282, NIH HL70755, and the 7th Framework Programme of the European Commission (EC-FP-7-NANOMMUNE-214281).

References

Aardema MJ, Albertini S, Arni P, Henderson LM, Kirsch-Volders M, Mackay JM, Sarrif AM, Stringer DA, Taalman RD. Aneuploidy: a report of an ECETOC task force. Mutat Res. 1998; 410(1):3–79. [PubMed: 9587424]

Allen BL, Kotchey GP, Chen Y, Yanamala NV, Klein-Seetharaman J, Kagan VE, Star A. Mechanistic investigations of horseradish peroxidase-catalyzed degradation of single-walled carbon nanotubes. J Am Chem Soc. 2009; 131(47):17194–17205. [PubMed: 19891488]

Arepalli S, Nikolaev P, Gorelik O. Analytical characterization of single wall carbon nanotubes. Encyclopedia of Nanoscience and Nanotechnology. 2004; V1:51–66.

Asakura M, Sasaki T, Sugiyama T, Takaya M, Koda S, Nagano K, Arito H, Fukushima S. Genotoxicity and cytotoxicity of multi-wall carbon nanotubes in cultured Chinese hamster lung cells in comparison with chrysotile A fibers. J Occup Health. 2010; 52(3):155–166. [PubMed: 20379079]

Bard D, Yarwood J, Tylee B. Asbestos fibre indentification by Raman microspectroscopy. J Raman Spectroscopy. 1997; 28:803–809.

Birch, ME. NIOSH Manual of Analytical Methods (NMAM 5040). 4. Vol. Chapter Q. NIOSH; Cincinnati, OH: 2003. Elemental Carbon. Monitoring of diesel exhaust particulate in the workplace. DHHS publication No 2003–154

Bronikowski MJ, Willis PA, Colbert DT, Smith KA, Smalley RE. Gasphase production of carbon single-walled nanotubes from carbon monoxide via the HiPco process: A parametric study. J Vac Sci Technol. 2001; 19:1800.

Brown DM, Kinloch IA, Bangert U, Windle A, Walter DM, Walker GS, Scotchford CA, Donaldson K, Stone V. An in vitro study of the potential of carbon nanotubes and nanofibres to induce inflammatory mediators and frustrated phagocytosis. Carbon. 2007; 45 (9):1743–1756.

Cveticanin J, Joksic G, Leskovac A, Petrovic S, Sobot AV, Neskovic O. Using carbon nanotubes to induce micronuclei and double strand breaks of the DNA in human cells. Nanotechnology. 2010; 21(1):015102. [PubMed: 19946169]

Darne C, Terzetti F, Coulais C, Fournier J, Guichard Y, Gaté L, Binet S. In vitro cytotoxicity and transforming potential of industrial carbon dust (fibers and particles) in syrian hamster embryo (SHE) cells. Ann Occup Hyg. 2010; 54(5):532–544. [PubMed: 20219837]

Decordier I, Dillen L, Cundari E, Kirsch-Volders M. Elimination of micronucleated cells by apoptosis after treatment with inhibitors of microtubules. Mutagenesis. 2002; 17(4):337–344. [PubMed: 12110631]

Ding M, Chen F, Shi X, Yucesoy B, Mossman B, Vallyathan V. Diseases caused by silica: mechanisms of injury and disease development. Int Immunopharmacol. 2002; 2:173–182. [PubMed: 11811922]

Doak SH, Griffiths SM, Manshian B, Singh N, Williams PM, Brown AP, Jenkins GJS. Confounding experimental considerations in nanogenotoxicology. Mutagenesis. 2009; 24:285–293. [PubMed: 19351890]

Dopp E, Schuler M, Schiffmann D, Eastmond DA. Induction of micronuclei, hyperdiploidy and chromosomal breakage affecting the centric/pericentric regions of chromosomes 1 and 9 in human amniotic fluid cells after treatment with asbestos and ceramic fibers. Mutat Res. 1997; 377(1):77–87. [PubMed: 9219582]

Dresselhaus, MS.; Dresselhaus, G.; Pimenta, MA.; Eklund, PC. Raman scattering in carbon materials. In: Pelletier, MJ., editor. Analytical Application of Raman Spectroscopy. Vol. Chapter 9. Blackwell; London, UK: 1999.

Dresselhaus MS, Dresselhaus G, Charlier JC, Hernandez E. Electronic, thermal and mechanical properties of carbon nanotubes. Philos Transact Ser A Math Phys Eng Sci. 2004; 362:2065–2098.

Gorelik, O.; Nikolaev, P.; Arepalli, S. Purification procedures for single-walled carbon nanotubes, NASA contractor report, NASA/CR-2000–208926. 2000.

Grabinski C, Hussain S, Lafdi K, Braydich-Stolle L, Schlager J. Effect of particle dimension on biocompatibility of carbon nanomaterials. Carbon. 2007; 45:2828–2835.

Goodglick LA, Kane AB. Role of reactive oxygen metabolites in crocidolite asbestos toxicity to mouse macrophages. Cancer Res. 1986; 46(11):5558–5566. [PubMed: 3019528]

Hill IM, Beswick PH, Donaldson K. Differential release of superoxide anions by macrophages treated with long and short fibre amosite asbestos is a consequence of differential affinity for opsonin. Occup Environ Med. 1995; 52(2):92–96. [PubMed: 7757173]

Hubbard R, Venn A, Lewis S, Britton J. Lung cancer and cryptogenic fibrosing alveolitis. A population-based cohort study. Am J Respir Crit Care Med. 2000; 161(1):5–8. [PubMed: 10619790]

Iarmarcovai G, Botta A, Orsière T. Number of centromeric signals in micronuclei and mechanisms of aneuploidy. Toxicol Lett. 2006; 166(1):1–10. [PubMed: 16854538]

ISO/TS 27687:2008. Nanotechnologies: Terminology and definitions for nano-object; nanoparticle, nanofibre and nanoplate. 2008.

Jacobsen NR, Pajana G, White P, Moller P, Cohn CA, Korsholm KS, Vogel U, Marcomini A, Loft S, Wallin H. Genotoxicity, cytotoxicity, and reactive oxygen species induced by single-walled carbon nanotubes and C (60) fullerenes in the FEl-Mutatrade markMouse lung epithelial cells. Environ Mol Mutagen. 2008; 49:476–487. [PubMed: 18618583]

Kagan VE, Tyurina YY, Tyurin VA, Konduru NV, Potapovich AI. Direct and indirect effects of single walled carbon nanotubes on RAW 264.7 macrophages: Role of iron. Toxicol Lett. 2006; 165:88–100. [PubMed: 16527436]

Kagan VE, Konduru NV, Feng W, Allen BL, Conroy J, Volkov Y, Vlasova II, Belikova NA, Yanamala N, Kapralov A, Tyurina YY, Shi J, Kisin ER, Murray AR, Franks J, Stolz D, Gou P, Klein-Seetharaman J, Fadeel B, Star A, Shvedova AA. Carbon nanotubes degraded by neutrophil myeloperoxidase induce less pulmonary inflammation. Nat Nanotechnol. 2010; 5(5):354–459. [PubMed: 20364135]

Kirsch-Volders M, Vanhauwaert A, De Boeck M, Decordier I. Importance of detecting numerical versus structural chromosome aberrations. Mutat Res. 2002; 504:137–148. [PubMed: 12106654]

Kisin ER, Murray AR, Keane MJ, Shi XC, Schwegler-Berry D, Gorelik O, Arepalli S, Castranova V, Wallace WE, Kagan VE, Shvedova AA. Single-walled carbon nanotubes: geno- and cytotoxic effects in lung fibroblast V79 cells. J Toxicol Environ Health A. 2007; 70(24):2071–2079. [PubMed: 18049996]

Knaapen AM, Borm PJA, Albrecht C, Schins RPF. Inhaled particles and lung cancer. Part A: Mechanisms. Int J Cancer. 2004; 109:799–809. [PubMed: 15027112]

Ku BK, Emery MS, Maynard AD, Stolzenburg M, McMurry PH. In situ structure characterization of airborne carbon nanofibers by a tandem mobility-mass analysis. Nanotechnology. 2006; 17:3613–3621. [PubMed: 19661613]

Li S, He P, Dong J, Guo Z, Dai L. DNA-directed self-assembling of carbon nanotubes. J Am Chem Soc. 2005; 127(1):14–15. [PubMed: 15631425]

Li X, Peng Y, Qu X. Carbon nanotubes selective destabilization of duplex and triplex DNA, inducing B-A transition in solution. Nucleic Acids Res. 2006; 34:3670–3676. [PubMed: 16885240]

Lindberg HK, Falck GC, Suhonen S, Vippola M, Vanhala E, Catalán J, Savolainen K, Norppa H. Genotoxicity of nanomaterials: DNA damage and micronuclei induced by carbon nanotubes and graphite nanofibres in human bronchial epithelial cells in vitro. Toxicol Lett. 2009; 186(3):166–173. [PubMed: 19114091]

Magrez A, Kasas S, Salicio V, Pasquier N, Won Seo J, Celio M, Catsicas S, Schwaller B, Forró L. Cellular toxicity of carbon-based nanomaterials. Nano Lett. 2006; 6 (6):1121–1125. [PubMed: 16771565]

Manning CB, Vallyathan V, Mossman BT. Diseases caused by asbestos: mechanisms of injury and disease development. Int Immunopharmacol. 2002; 2:191–200. [PubMed: 11811924]

Mateuca R, Lombaert N, Aka PV, Decordier I, Kirsch-Volders M. Chromosomal changes: induction, detection methods and applicability in human biomonitoring. Biochimie. 2006; 88:1515–1531. [PubMed: 16919864]

Maynard AD, Ku BK, Emery M, Stolzenburg M, McMurry P. Measuring particle size-dependent physicochemical structure in airborne single walled carbon nanotube agglomerates. J Nanoparticle Res. 2007; 9:85–92.

Msiska Z, Pacurari M, Mishra A, Leonard SS, Castranova V, Vallyathan V. DNA Double-Strand Breaks by Asbestos, Silica, and Titanium Dioxide. Possible Biomarker of Carcinogenic Potential? Am J Respir Cell and Mol Biol. 2010; 43:210–219. [PubMed: 19783790]

Muller J, Decordier I, Hoet PH, Lombaert N, Thomassen L, Huaux F, Lison D, Kirsch-Volders M. Clastogenic and aneugenic effects of multi-wall carbon nanotubes in epithelial cells. Carcinogenesis. 2008; 29(2):427–433. [PubMed: 18174261]

Pacurari M, Yin XJ, Zhao J, Ding M, Leonard SS, Schwegler-Berry D, Ducatman BS, Sbarra D, Hoover M, Castranova V, Vallyathan V. Raw single-wall carbon nanotubes induce oxidative stress an activate MAPKs, AP-1, NF-KB, and Akt in normal and malignant human mesothelial cells. Environ Health Perspect. 2008a; 116:1211–1217. [PubMed: 18795165]

Pacurari M, Yin XJ, Ding M, Leonard SS, Schwegler-Berry D, Ducatman BS, Chirila M, Endo M, Castranova V, Vallyathan V. Oxidative and molecular interactions of multi-wall carbon nanotubes (MWCNT) in normal and malignant human mesothelial cells. Nanotoxicology. 2008b; 2(3):155–170.

Pantarotto D, Briand JP, Prato M, Bianco A. Translocation of bioactive peptides across cell membranes by carbon nanotubes. Chem Commun (Camb). 2004; 1:16–17. [PubMed: 14737310]

Patlolla A, Knighten B, Tchounwou P. Multi-walled carbon nanotubes induce cytotoxicity, genotoxicity and apoptosis in normal human dermal fibroblast cells. Ethn Dis. 2010; 20(1):S1, 65–72. [PubMed: 20521388]

Pietruska JR, Johnston T, Zhitkovich A, Kane AB. XRCC1 deficiency sensitizes human lung epithelial cells to genotoxicity by crocidolite asbestos and libby amphibole. Environ Health Perspect. 2010 [Epub ahead of print].

Poland CA, Duffin R, Kinloch I, Maynard A, Wallace WA, Seaton A, Stone V, Brown S, Macnee W, Donaldson K. Carbon nanotubes introduced into the abdominal cavity of mice show asbestos-like pathogenicity in a pilot study. Nat Nanotechnol. 2008; 3(7):423–428. [PubMed: 18654567]

Price RL, Haberstroh KM, Webster TJ. Improved osteoblast viability in the presence of smaller nanometre dimensioned carbon fibres. Nanotechnology. 2004; 15(8):92.

Rinaudo C, Belluso E, Gastaldi D. Assessment of the use of Raman spectroscopy for the determination of amphibole asbestos. Mineralogical Magazine. 2004; 68(3):455–465.

Sargent LM, Ensell MX, Ostvold AC, Baldwin KT, Kashon ML, Lowry DT, Senft JR, Jefferson AM, Johnson RC, Li Z, Tyson FL, Reynolds SH. Chromosomal changes in high- and low-invasive mouse lung adenocarcinoma cell strains derived from early passage mouse lung adenocarcinoma cell strains. Toxicol Appl Pharmacol. 2008; 233(1):81–91. [PubMed: 18367224]

Sargent LM, Shvedova AA, Hubbs AF, Salisbury JL, Benkovic SA, Kashon ML, Lowry DT, Murray AR, Kisin ER, Friend S, McKinstry KT, Battelli L, Reynolds SH. Induction of aneuploidy by single-walled carbon nanotubes. Environ Mol Mutagen. 2009; 50(8):708–717. [PubMed: 19774611]

Sargent LM, Reynolds SH, Castranova V. Potential pulmonary effects of engineered carbon nanotubes: in vitro genotoxic effects. Nanotoxicology. 2010:1–13. early online.

Schins RP. Mechanisms of genotoxicity of particles and fibers. Inhal Toxicol. 2002; 14(1):57–78. [PubMed: 12122560]

Schins RP, Knaapen AM. Genotoxicity of poorly soluble particles. Inhal Toxicol. 2007; 19 (Suppl 1): 189–198. [PubMed: 17886067]

Shvedova AA, Kagan VE, Fadeel B. Close encounters of the small kind: adverse effects of man-made materials interfacing with the nano-cosmos of biological systems. Annu Rev Pharmacol Toxicol. 2010; 50:63–88. [PubMed: 20055698]

Shvedova AA, Kisin ER, Porter D, Schulte P, Kagan VE, Fadeel B, Castranova V. Mechanisms of pulmonary toxicity and medical applications of carbon nanotubes: Two faces of Janus? Pharmacol Ther. 2009; 121(2):192–204. [PubMed: 19103221]

Shvedova AA, Kisin ER, Mercer R, Murray AR, Johnson VJ, Potapovich AI, Tyurina YY, Gorelik O, Arepalli S, Schwegler-Berry D, Hubbs AF, Antonini J, Evans DE, Ku BK, Ramsey D, Maynard A, Kagan VE, Castranova V, Baron P. Unusual inflammatory and fibrogenic pulmonary responses to single-walled carbon nanotubes in mice. Am J Physiol Lung Cell Mol Physiol. 2005; 289:L698–L708. [PubMed: 15951334]

Shukla A, Gulumian M, Hei TK, Kamp D, Rahman Q, Mossman BT. Multiple roles of oxidants in the pathogenesis of asbestos-induced diseases. Free Radic Biol Med. 2003; 34(9):1117–1129. [PubMed: 12706492]

Vallyathan V, Shi X, Castranova V. Reactive oxygen species: their relation to pneumoconiosis and carcinogenesis. Environ Health Perspect. 1998; 106(Suppl 5):1151–1155. [PubMed: 9788890]

Wang H, Feng JY, Hu XJ, Ng KM. Synthesis of aligned carbon nanotubes on double-sided metallic substrate by chemical vapor deposition. J Physical Chemistry C. 2007; 111(34):12617–12624.

Wang Y, Serrano S, Santiago-Aviles JJ. Raman characterization of carbon nanofibers prepared using electrospinning. Synthetic Metals. 2003; 138:423–427.

Wiley JE, Sargent LM, Inhorn SL, Meisner LF. Comparison of prometaphase chromosome techniques with emphasis on the role of colcemid. In Vitro. 1984; 20(12):937–941. [PubMed: 6530228]

Witasp E, Shvedova AA, Kagan VE, Fadeel B. Single-walled carbon nanotubes impair human macrophage engulfment of apoptotic cell corpses. Inhal Toxicol. 2009; 21(Suppl 1):131–136. [PubMed: 19558245]

Yamashita K, Yoshioka Y, Higashisaka K, Morishita Y, Yoshida T, Fujimura M, Kayamuro H, Nabeshi H, Yamashita T, Nagano K, Abe Y, Kamada H, Kawai Y, Mayumi T, Yoshikawa T, Itoh N, Tsunoda S. Carbon nanotubes elicit DNA damage and inflammatory response relative to their size and shape. Inflammation. 2010; 33(4):276–280. [PubMed: 20174859]

Yegles M, Janson X, Dong HY, Renier A, Jaurand MC. Role of fibre characteristics on cytotoxicity and induction of anaphase/telophase aberrations in rat pleural mesothelial cells *in vitro*. Correlations with *in vivo* animal findings. Carcinogenesis. 1995; 16:2751–2758. [PubMed: 7586195]

Zhu L, Chang DW, Dai L, Hong Y. DNA damage induced by multiwalled carbon nanotubes in mouse embryonic stem cells. Nano Lett. 2007; 7:3592–3597. [PubMed: 18044946]

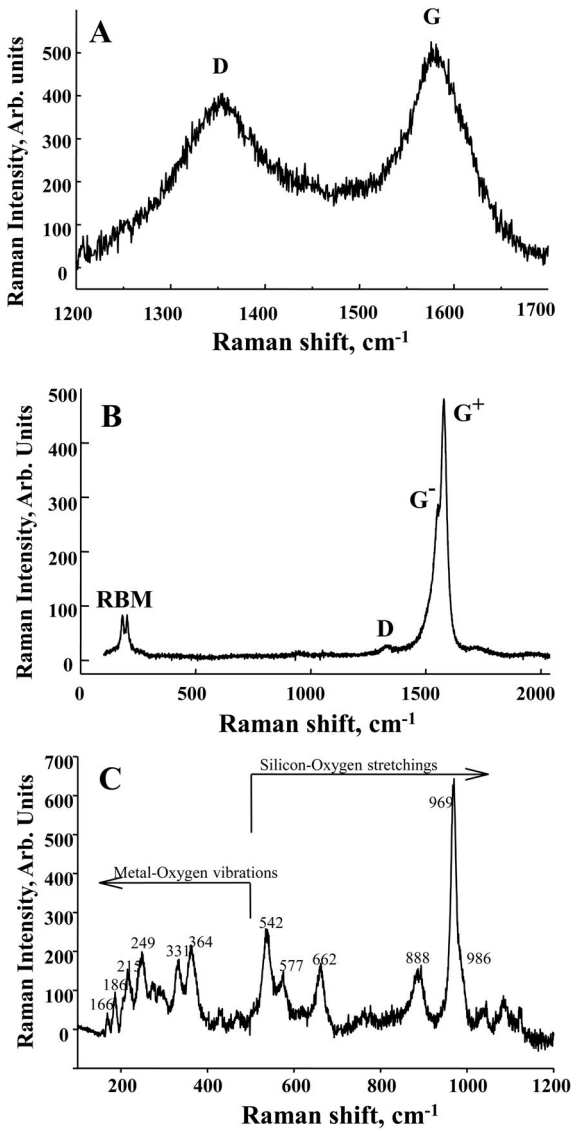

Figure 1.

Characterization of fibrous nanomaterials. Raman spectra from CNF (A), SWCNT (B), and crocidolite asbestos (C). For the graphite-based materials CNF and SWCNT there are two common features: D band at 1350 cm^{-1} due to amorphous carbon, impurities, and structural defects and G band at 1590 cm^{-1} due to high-ordered graphite structure. Low-frequency bands called radial breathing mode (RBM) are seen only in the SWCNT spectrum. The crocidolite spectrum shows specific bands due to metal – oxygen vibrations, below 500 cm^{-1} and to silicon – oxygen vibrations in the rest of the spectrum.

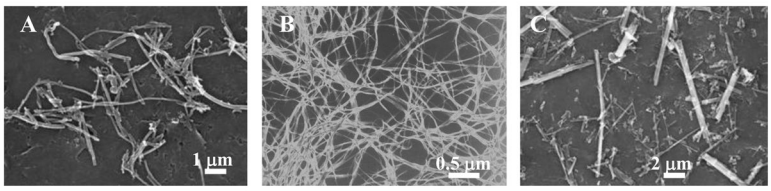

Figure 2.
Scanning electron microscopy images of CNF (A), SWCNT (B), and asbestos (C).

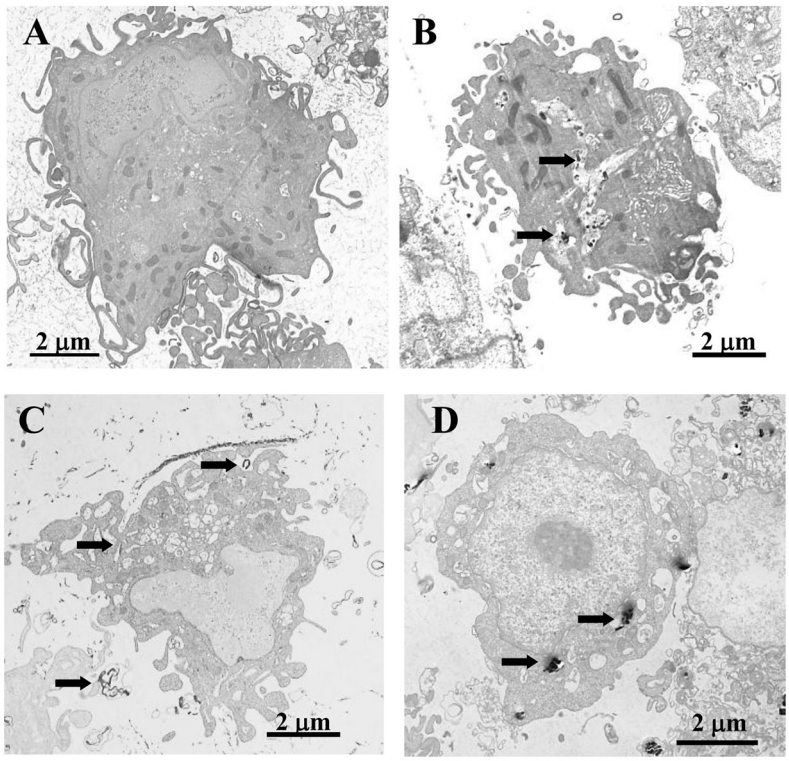

Figure 3.

Cellular uptake and ultra-structural effects of fibrous nanomaterials. Transmission electron micrographs of RAW264.7 macrophages after exposure to CNF (B), SWCNT (C) or asbestos (D). PBS-exposed control cells are shown in (A). RAW264.7 macrophages were incubated with 24 μg/cm^2 of CNF, asbestos or SWCNT for 24h (37°C). Arrows indicate engulfment of the particles.

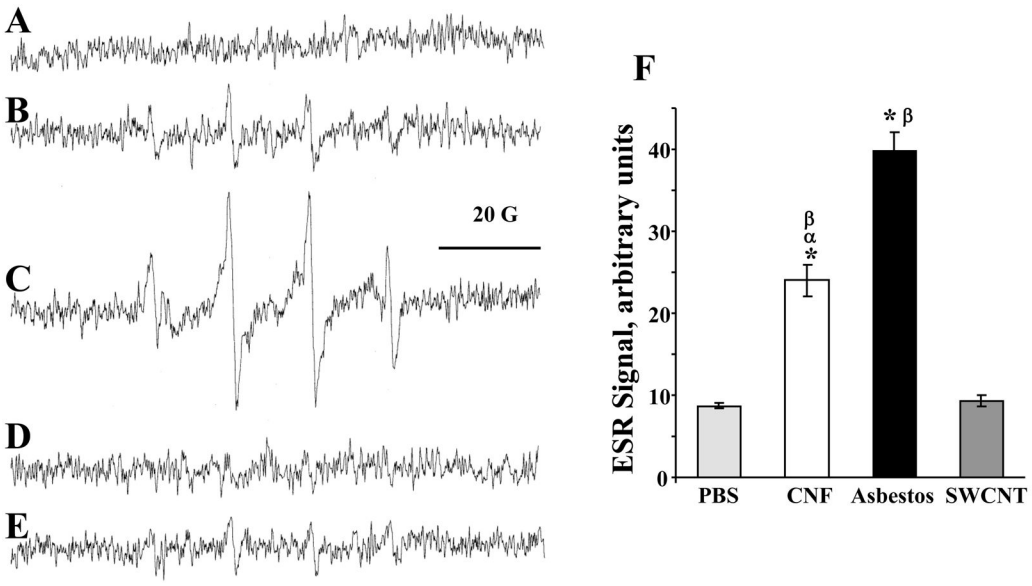

Figure 4.

ROS generation by fibrous nanomaterials. ESR detection of free radicals formed *in vitro* and spin-trapped with DMPO in RAW264.7 macrophages after exposure to CNF, SWCNT or asbestos. (A) RAW264.7 macrophages (1×10^6 cells/ml) in PBS (pH 7.4) plus 100 mM DMPO. (B) ESR spectra recorded 5 min after the addition of CNF (120 μg/ml) to RAW264.7 macrophages (1×10^6 cells/ml) in PBS (pH 7.4) plus DMPO (100 mM). (C) Same as B plus H_2O_2 (1 mM). (D) Same as B plus catalase (20 U/ml). (E) Same as B plus DFO (0.2 mM). (F) ESR signals generated by CNF, asbestos or SWCNT in RAW264.7 macrophages. Instrument conditions: microwave power, 20 mW; modulation amplitude, 1.0 G; time constant, 1.3 sec; conversion time, 0.6 sec. *$p<0.05$, vs control; $^{\alpha}p<0.05$, vs asbestos treated samples; $^{\beta}p<0.05$, vs SWCNT treated samples.

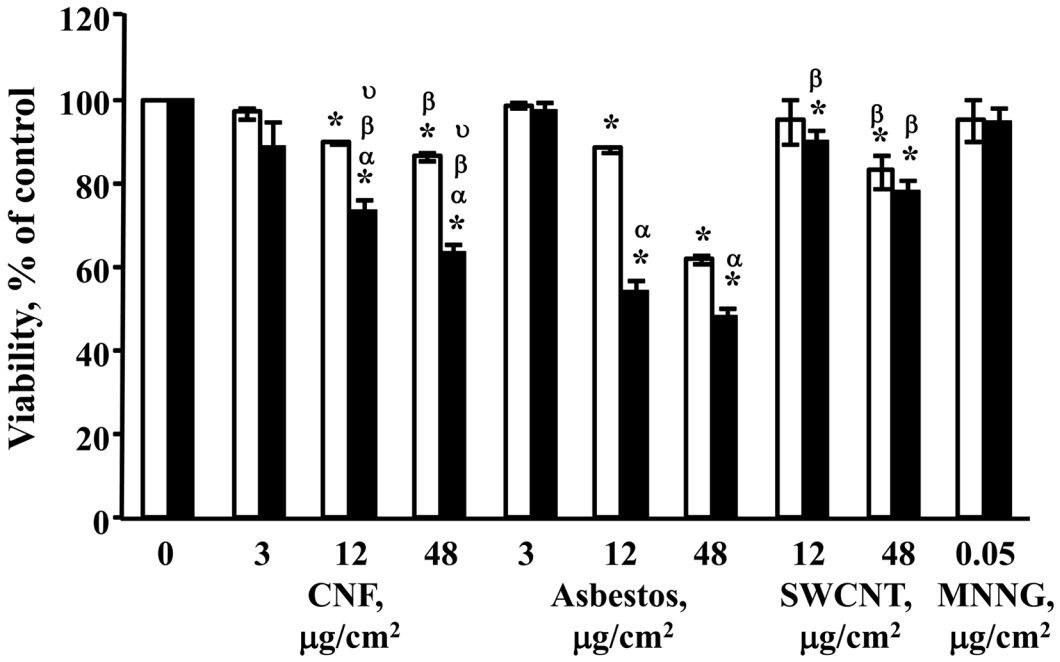

Figure 5.

Cytotoxicity of fibrous nanomaterials. Viability of V79 cells after 3 or 24 hr exposure to CNF, SWCNT or asbestos, as determined by trypan blue exclusion: □ - 3 hr exposure; ■ - 24 hr exposure. Data are shown as mean values ± SEM (n=3 experiments); *$p<0.05$ *vs.* control cells; $^{\alpha}p<0.05$ *vs.* exposure with the same material for 3 hr; $^{\beta}p<0.05$ *vs.* corresponding treatment (the same dose and time of exposure) with asbestos; $^{\upsilon}p<0.05$ *vs.* corresponding treatment (the same dose and time of exposure) with SWCNT. N-methyl-N-nitroso-N-nitrosoguanidine (MNNG) was used as a positive control for DNA damage.

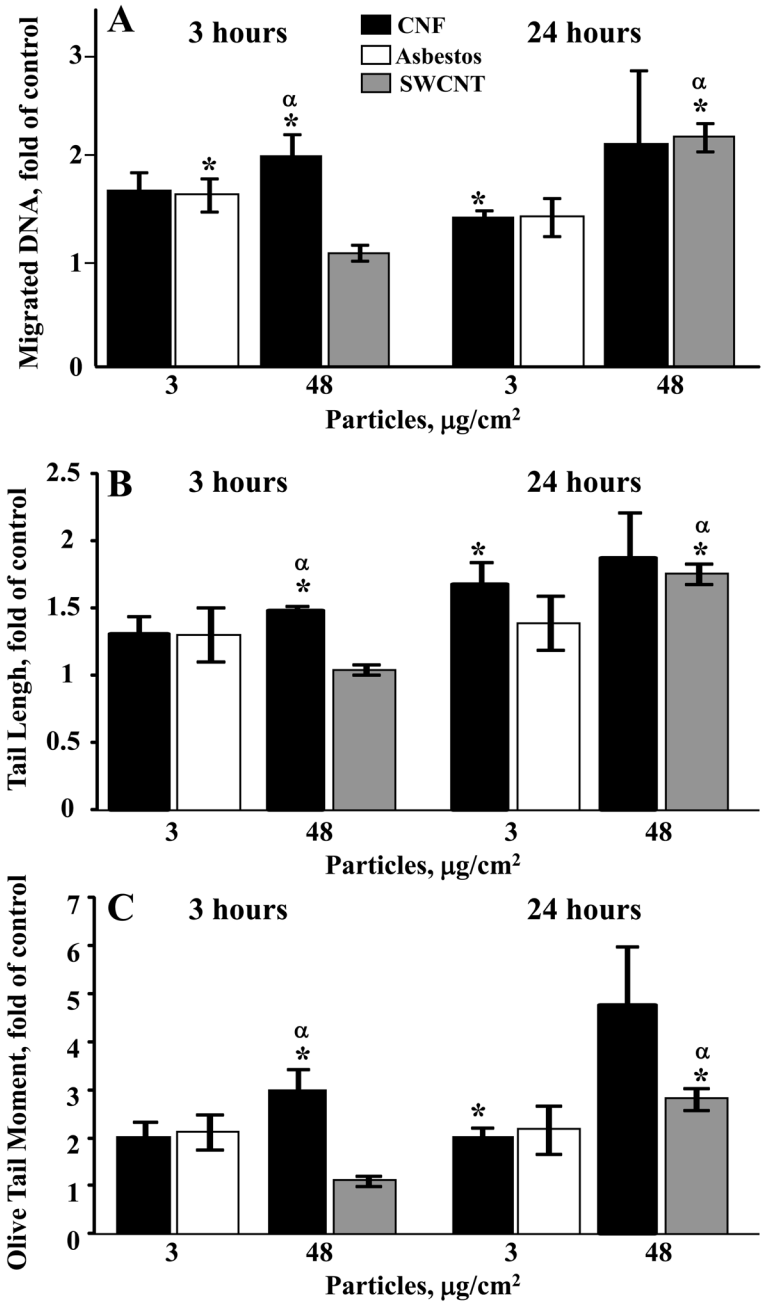

Figure 6.

DNA damage induced by fibrous nanomaterials. The comet assay was utilized to monitor DNA damage in V79 cells after challenge with CNF, SWCNT or asbestos: (A) DNA damage as migrated DNA; (B) DNA damage as tail lengh; (C) DNA damage as olive tail moment. ■ – exposure with CNF;↑ – exposure with asbestos, ▩ – exposure with SWCNT. *p<0.05, vs control; ᵅp<0.05, vs V79 cells treated with SWCNT for 3 hr. Data represent mean values ±SEM of the alkaline comet assay based on 100 cells/sample (n=3 experiments).

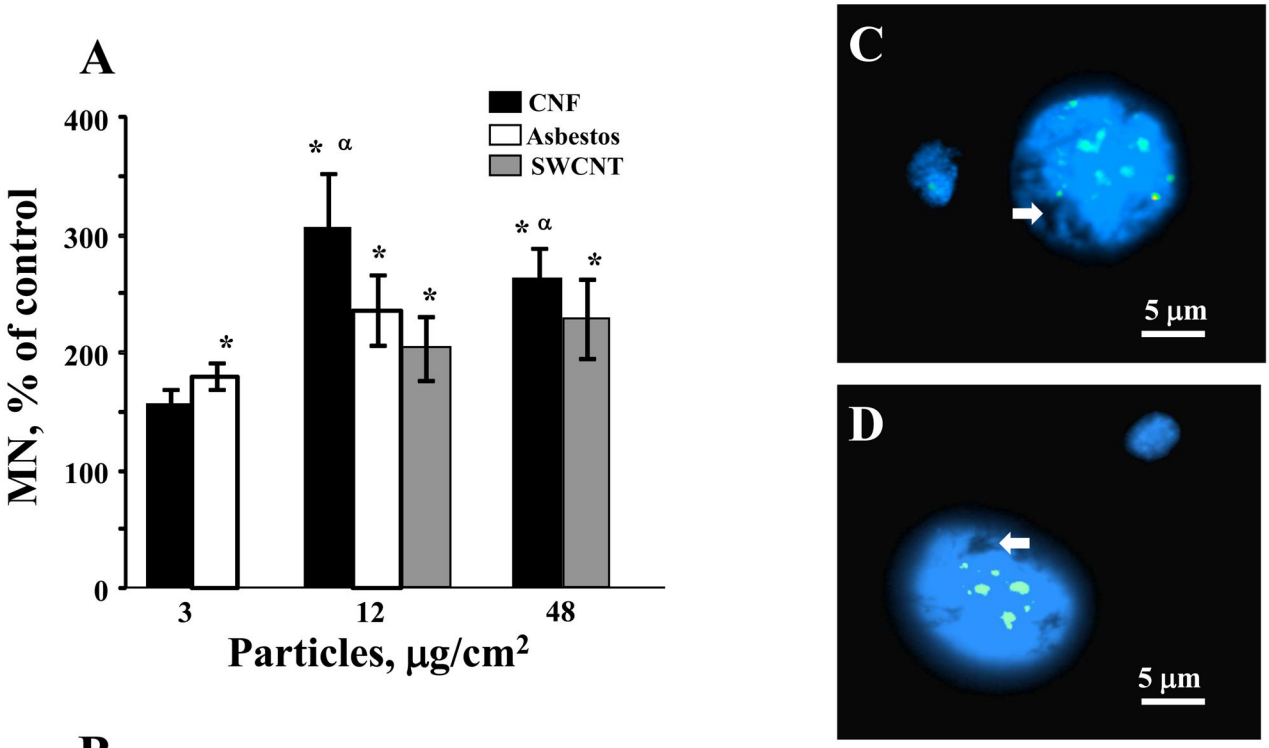

B

Aneugenic/Clastogenic events, %	CNF 2.4 μg/cm²	CNF 24 μg/cm²
Centromere-positive, %	83.5±6.01*	82.0±5.66*
Centromere-negative, %	16.5±6.72*	18.0±5.66*

Figure 7.

Chromosomal changes induced by fibrous nanomaterials: (A) Micronucleated cell induction in 1000 scored cells after challenge with CNF, SWCNT or asbestos in V79 cells. ■ – exposure with CNF; ↑ – exposure with asbestos, ▩ – exposure with SWCNT. Data are shown as mean values ± SEM (n=3 experiments); *p<0.05, vs control; $^{\alpha}$p<0.05, vs 3 μg/cm^2 of the same treatment. (B) Number of centromere-positive and centromere-negative MN in SEAC incubated with CNF (2.4 and 24 μg/cm^2). Data are shown as mean values ± SEM; *p<0.05, vs control. (C) Centromere-positive (aneugenic) and (D) centromere-negative (clastogenic) MN after exposure to 2.4 mg/cm^2 CNF. Arrows indicate CNF within a nucleus.

Table 1

Physico-chemical characteristics of the tested materials.

	CNF (Pyrograf III)	Crocidolite Asbestos	SWCNT
Iron content, %	1.4	18	0.23
Surface area, m^2/g	35 – 45	8.3	1040
Diameter, nm	60 – 150	210	1 – 4
Aspect ratio (median)	500	30	1000
Integral intensity ratio [a] $R=I_D/I_G$	0.95	N/A	0.05
Graphite mole fraction [a] $\chi_G = 1/(1+R)$	0.51	N/A	0.95

[a] Raman spectroscopy